

Supporting materials for:

**Ternary PtFeCo Alloys on Graphene with Highly Electrocatalytic
Activities for Methanol Oxidation**

Hongfei Wang¹, Kefu Zhang¹, Jun Qiu¹, Juan Wu¹, Jingwen Shao¹, Huijuan Wang¹,
Yujuan Zhang², Jie Han², Yong Zhang³, Lifeng Yan^{1,*}

¹CAS Key Laboratory of Soft Matter Chemistry, Hefei National Laboratory for
Physical Sciences at the Microscale, and Department of Chemical Physics, University
of Science and Technology of China, Hefei, 230026, P.R.China

² Yanchang Petroleum (Group) Co.,Ltd., No.61 Tangyan Rd, Xi'an, Shaanxi,
P.R.China 710065

³The Northwest Research Institute of Chemical Industry Co.,Ltd, Xi'an, Shaanxi,
710061, P.R.China

Table S1. The inductively coupled plasma atomic emission spectroscopy (ICP-AES) results for all samples.

Samples	Mass%	Elements	Atom%	Atom%
	(Pt, ICP-AES)		(feeding	(ICP-AES)
			ratio)	
Pt₃₀Fe₃₇Co₃₃@G-7%	6.85%	Pt:Fe:Co	32:34:34	30:37:33
Pt₅₂Fe₂₉Co₁₉@G-7%	6.93%	Pt:Fe:Co	50:25:25	52:29:19
Pt₆₄Fe₂₀Co₁₆@G-7%	7.09%	Pt:Fe:Co	70:15:15	64:20:16
Pt₅₈Fe₄₂@G-7%	6.87%	Pt:Fe	50:50	58:42
Pt₅₂Co₄₈@G-7%	6.72%	Pt:Co	50:50	52:48
Pt₄₈Fe₂₅Co₂₇@G-10%	9.88%	Pt:Fe:Co	50:25:25	48:25:27
Pt₅₁Fe₂₇Co₂₂@G-4%	4.11%	Pt:Fe:Co	50:25:25	51:27:22
Pt₅₀Fe₂₈Co₂₂@G-1%	1.03%	Pt:Fe:Co	50:25:25	50:28:22

Table S2. XRD values of all PtFeCo@G-7% samples.

Samples	2θ/degree e (111)	Experimental lattice parameter	Theoretica lattice parameter	d ₍₁₁₁₎ spacing (Å)	Strain (%)
Pt (JCPDS No. 04-0802)	39.76	3.923		0.2265	
Pt ₃₀ Fe ₃₇ Co ₃₃ @G- 7%	41.10	3.795	3.407	0.2191	3.27
Pt ₅₂ Fe ₂₉ Co ₁₉ @G- 7%	40.66	3.838	3.545	0.2216	2.16
Pt ₆₄ Fe ₂₀ Co ₁₆ @G- 7%	40.48	3.862	3.651	0.2230	1.55

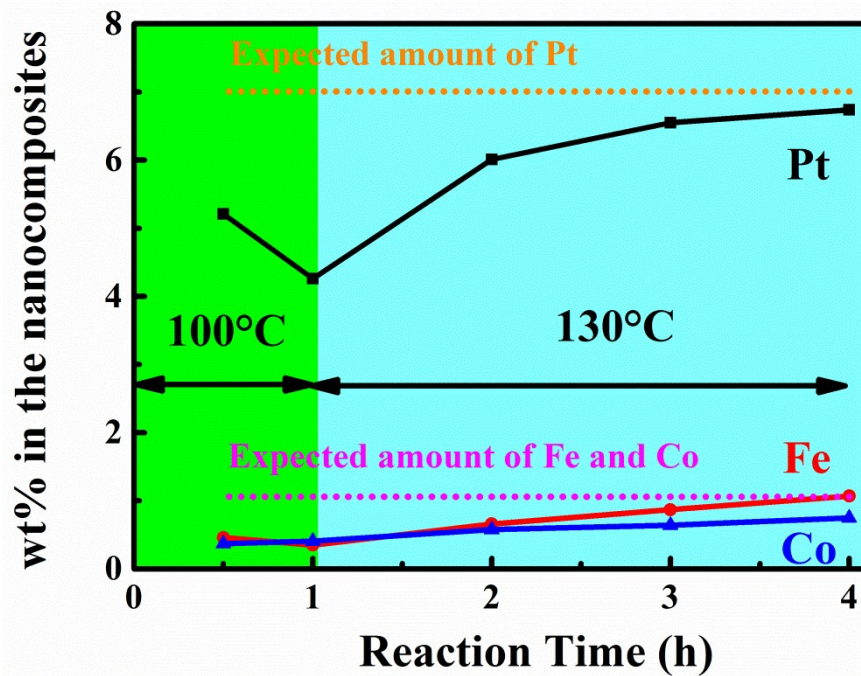


Figure S1. the elemental weight composition of $\text{Pt}_{52}\text{Fe}_{29}\text{Co}_{19}@\text{G}-7\%$ as a function of the reaction time.

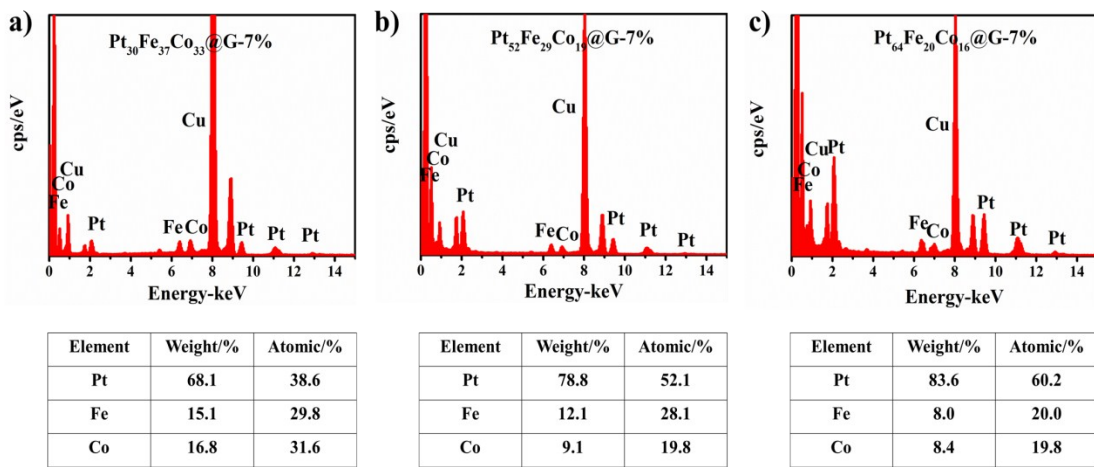


Figure S2. EDX-area analyses of (a) $\text{Pt}_{30}\text{Fe}_{37}\text{Co}_{33}@\text{G-7\%}$, (b) $\text{Pt}_{52}\text{Fe}_{29}\text{Co}_{19}@\text{G-7\%}$, and (c) $\text{Pt}_{64}\text{Fe}_{20}\text{Co}_{16}@\text{G-7\%}$ nanocomposites.

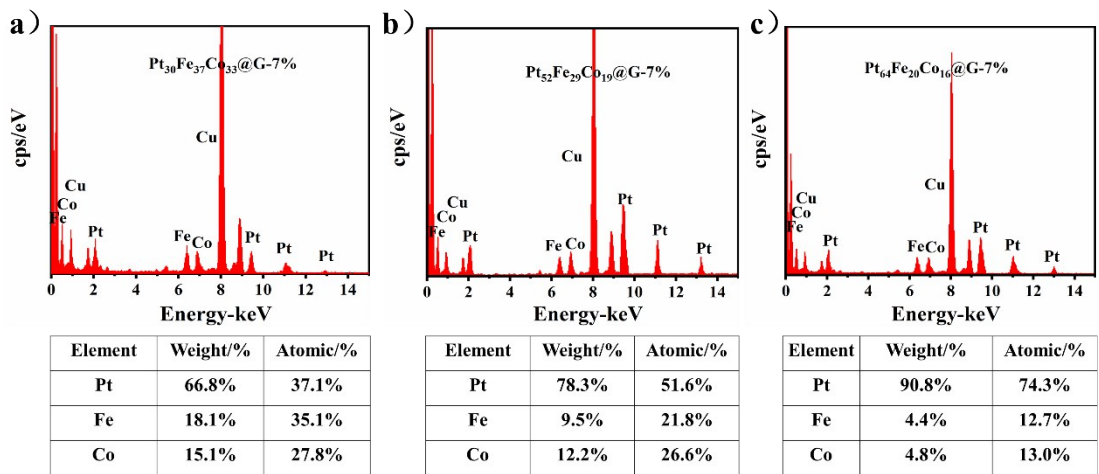


Figure S3. EDX-particle analyses of (a) $\text{Pt}_{30}\text{Fe}_{37}\text{Co}_{33}@\text{G-7\%}$, (b) $\text{Pt}_{52}\text{Fe}_{29}\text{Co}_{19}@\text{G-7\%}$, and (c) $\text{Pt}_{64}\text{Fe}_{20}\text{Co}_{16}@\text{G-7\%}$ nanocomposites.

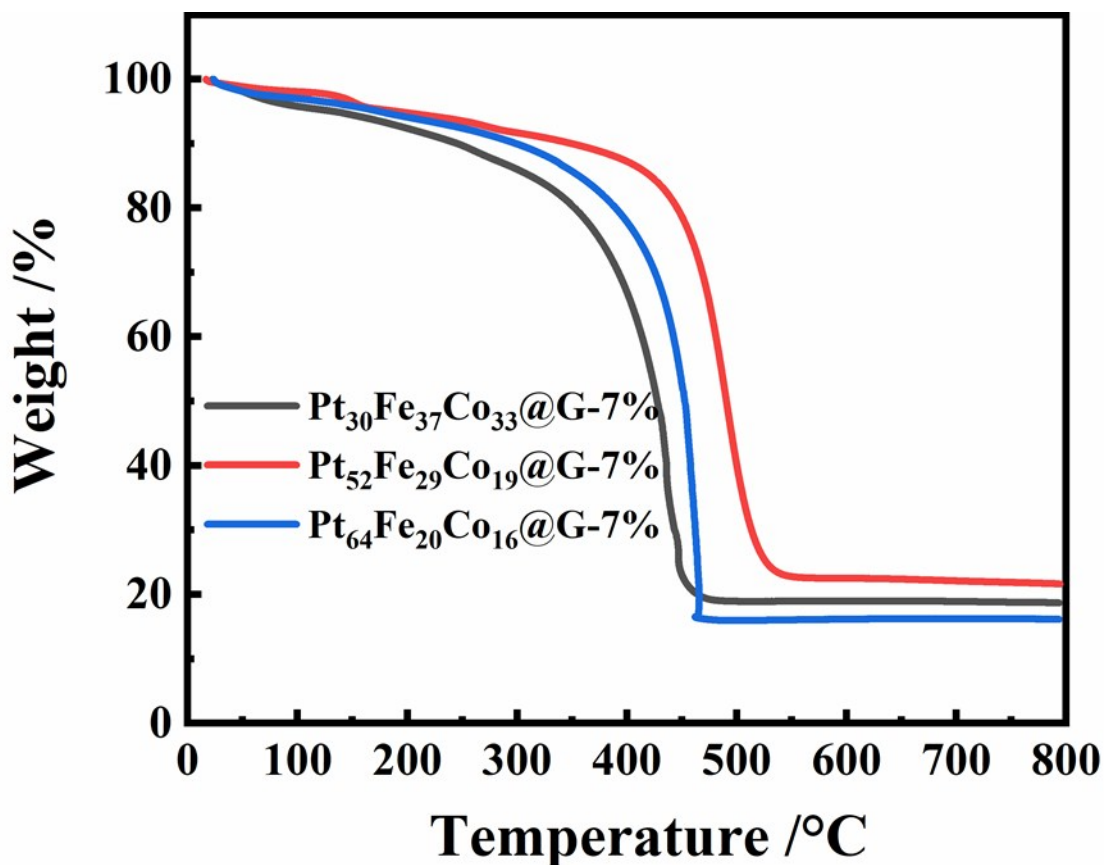


Figure S4. TGA curves of Pt₃₀Fe₃₇Co₃₃@G-7%, Pt₅₂Fe₂₉Co₁₉@G-7%, and Pt₆₄Fe₂₀Co₁₆@G-7% nanocomposites.

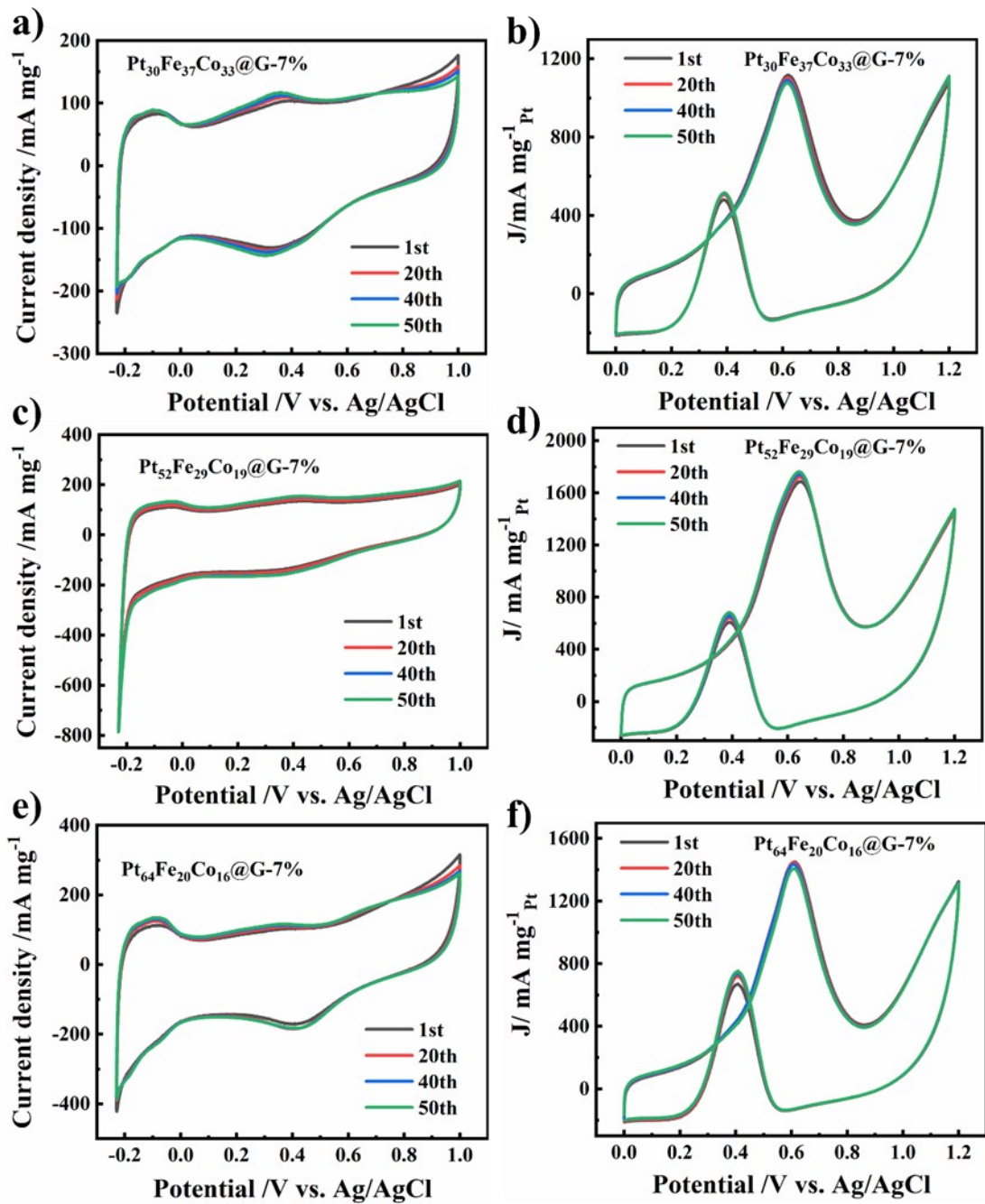


Figure S5. CV curves of (a) $\text{Pt}_{30}\text{Fe}_{37}\text{Co}_{33}@\text{G-7\%}$, (c) $\text{Pt}_{52}\text{Fe}_{29}\text{Co}_{19}@\text{G-7\%}$, (e)

$\text{Pt}_{64}\text{Fe}_{20}\text{Co}_{16}@\text{G-7\%}$ electrodes in 0.5 M H_2SO_4 at 50 mV s⁻¹ from the 1st circle to the

50th circle; CV curves of (b) $\text{Pt}_{30}\text{Fe}_{37}\text{Co}_{33}@\text{G-7\%}$, (d) $\text{Pt}_{52}\text{Fe}_{29}\text{Co}_{19}@\text{G-7\%}$, (f)

$\text{Pt}_{64}\text{Fe}_{20}\text{Co}_{16}@\text{G-7\%}$ electrodes in 0.5 M $\text{H}_2\text{SO}_4 + 0.5$ M CH_3OH at 50 mV s⁻¹ from

the 1st circle to the 50th circle.

Table S3. The onset potentials and peak potentials of CO oxidation for $\text{Pt}_{30}\text{Fe}_{37}\text{Co}_{33}@\text{G}$ -7%, $\text{Pt}_{52}\text{Fe}_{29}\text{Co}_{19}@\text{G}$ -7%, $\text{Pt}_{64}\text{Fe}_{20}\text{Co}_{16}@\text{G}$ -7% and Pt/C

	onset potential of CO oxidation (V)	peak potential of CO oxidation (V)
$\text{Pt}_{30}\text{Fe}_{37}\text{Co}_{33}@\text{G-}$ 7%	0.44	0.57
$\text{Pt}_{52}\text{Fe}_{29}\text{Co}_{19}@\text{G-}$ 7%	0.40	0.56
$\text{Pt}_{64}\text{Fe}_{20}\text{Co}_{16}@\text{G-}$ 7%	0.45	0.60
Pt/C	0.50	0.66

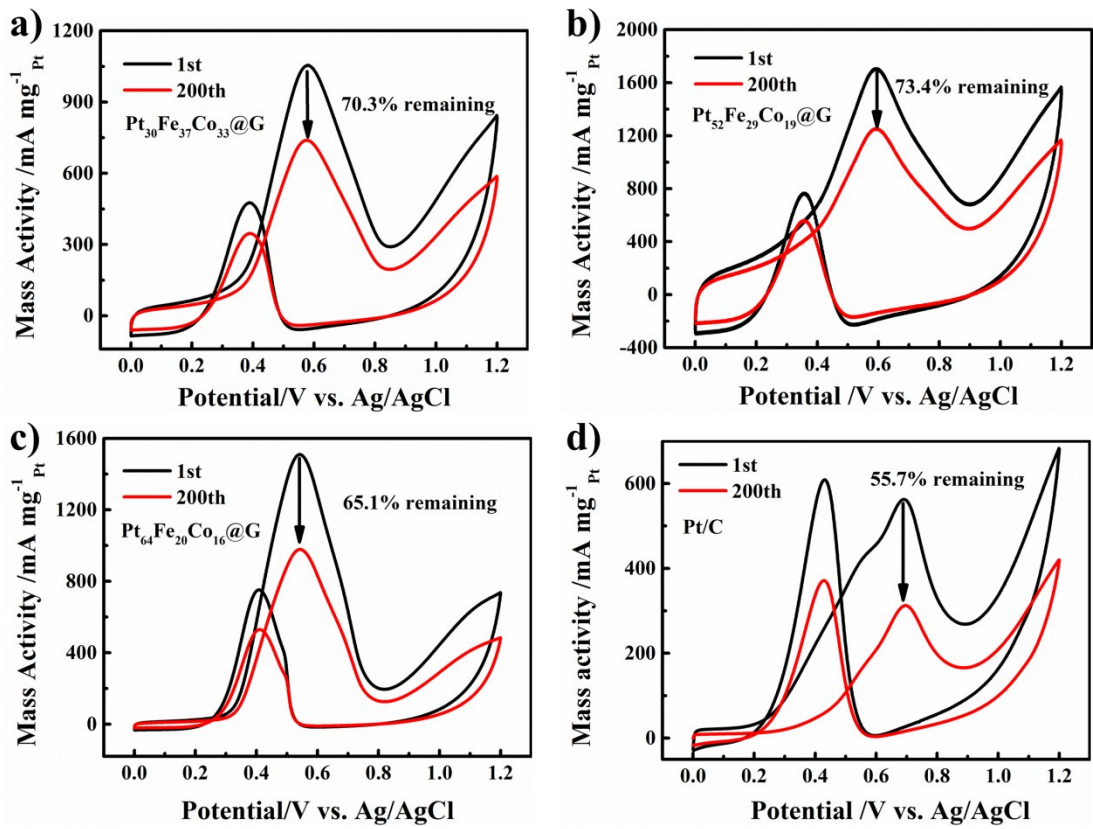


Figure S6. CV curves recorded at a sweep rate of 50 mV s⁻¹ in 0.5 M H₂SO₄ and 0.5 M CH₃OH aqueous solution for the 1st and 200th cycles.

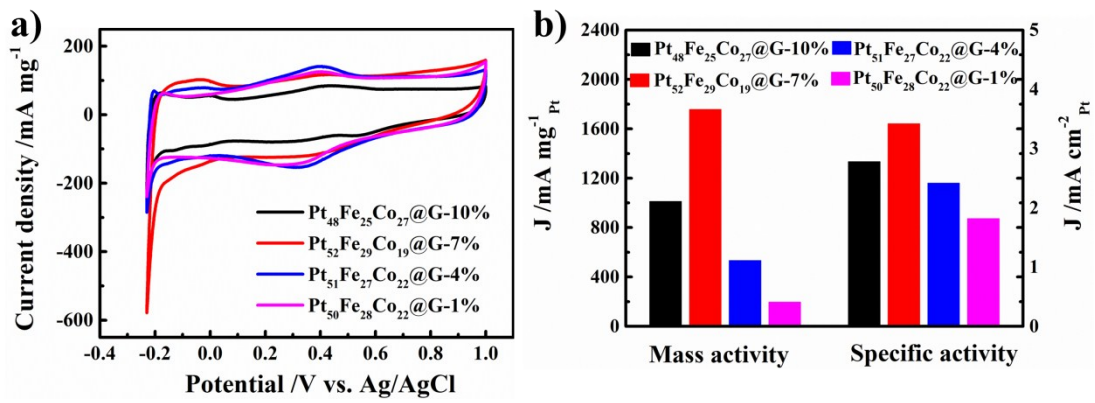


Figure S7. (a) CV curves of Pt₄₈Fe₂₅Co₂₇@G-10%, Pt₅₂Fe₂₉Co₁₉@G-7%, Pt₅₁Fe₂₇Co₂₂@G-4% and Pt₅₀Fe₂₈Co₂₂@G-1% electrodes in 0.5 M H₂SO₄ at a scan rate of 50 mV s⁻¹; (b) Bar graph illuminating the mass activities (left) and specific activities (right) at anodic peak potential.